

ORIGINAL RESEARCH

Retinol-Binding Protein 4 Promotes Cardiac Injury After Myocardial Infarction Via Inducing Cardiomyocyte Pyroptosis Through an Interaction With NLRP3

Kang-Zhen Zhang, PhD*¹; Xi-Yu Shen, PhD*¹; Man Wang, MD*¹; Li Wang, PhD¹; Hui-Xian Sun, MD¹; Xiu-Zhen Li, PhD¹; Jing-Jing Huang ¹, PhD¹; Xiao-Qing Li, MD¹; Cheng Wu, MD¹; Can Zhao, PhD¹; Jia-Li Liu, PhD¹; Xiang Lu, MD, PhD¹; Wei Gao ¹, MD, PhD¹

BACKGROUND: Acute myocardial infarction (AMI) is one of the leading causes of cardiovascular morbidity and mortality worldwide. Pyroptosis is a form of inflammatory cell death that plays a major role in the development and progression of cardiac injury in AMI. However, the underlying mechanisms for the activation of pyroptosis during AMI are not fully elucidated.

METHODS AND RESULTS: Here we show that RBP4 (retinol-binding protein 4), a previous identified proinflammatory adipokine, was increased both in the myocardium of left anterior descending artery ligation-induced AMI mouse model and in ischemia-hypoxia-induced cardiomyocyte injury model. The upregulated RBP4 may contribute to the activation of cardiomyocyte pyroptosis in AMI because overexpression of RBP4 activated NLRP3 (nucleotide-binding oligomerization domain-like receptor family pyrin domain-containing 3) inflammasome, promoted the precursor cleavage of Caspase-1, and subsequently induced GSDMD (gasdermin-D)-dependent pyroptosis. In contrast, knockdown of RBP4 alleviated ischemia-hypoxia-induced activation of NLRP3 inflammasome signaling and pyroptosis in cardiomyocytes. Mechanistically, coimmunoprecipitation assay showed that RBP4 interacted directly with NLRP3 in cardiomyocyte, while genetic knockdown or pharmacological inhibition of NLRP3 attenuated RBP4-induced pyroptosis in cardiomyocytes. Finally, knockdown of RBP4 in heart decreased infarct size and protected against AMI-induced pyroptosis and cardiac dysfunction in mice.

CONCLUSIONS: Taken together, these findings reveal RBP4 as a novel modulator promoting cardiomyocyte pyroptosis via interaction with NLRP3 in AMI. Therefore, targeting cardiac RBP4 might represent a viable strategy for the prevention of cardiac injury in patients with AMI.

Key Words: acute myocardial infarction ■ ischemia-hypoxia ■ NLRP3 ■ pyroptosis ■ retinol-binding protein 4

Acute myocardial infarction (AMI) is a severe and long-lasting ischemia of the myocardium caused by a sudden reduction or interruption of the coronary blood supply, leading to myocardial necrosis.¹ AMI is one of the leading causes of cardiovascular morbidity and mortality worldwide because of the serious clinical complications.¹ Pyroptosis, a newly identified form of

proinflammatory programmed cell death, is characterized by the cleavage of pore-forming protein GSDMD (gasdermin-D) and the formation of cytotoxic pores in the plasma membrane.² The activation of NLRP3 (nucleotide-binding oligomerization domain-like receptor family pyrin domain-containing 3) inflammasome promotes the precursor cleavage of Caspase-1, which

Correspondence to: Wei Gao, MD, PhD, and Xiang Lu, MD, PhD, Department of Geriatrics, Sir Run Run Hospital, Nanjing Medical University, Nanjing 211166, China. E-mails: gaowei84@njmu.edu.cn; luxiang66@njmu.edu.cn

*K.-Z. Zhang, X.-Y. Shen, and M. Wang contributed equally.

Supplementary Material for this article is available at <https://www.ahajournals.org/doi/suppl/10.1161/JAHA.121.022011>

For Sources of Funding and Disclosures, see page 15.

© 2021 The Authors. Published on behalf of the American Heart Association, Inc., by Wiley. This is an open access article under the terms of the Creative Commons Attribution-NonCommercial-NoDerivs License, which permits use and distribution in any medium, provided the original work is properly cited, the use is non-commercial and no modifications or adaptations are made.

JAHA is available at: www.ahajournals.org/journal/jaha

CLINICAL PERSPECTIVE

What Is New?

- Our present study demonstrated that RBP4 (retinol-binding protein 4), a previously identified proinflammatory adipokine, was increased in the myocardium of acute myocardial infarction mouse model and ischemia/hypoxia-induced cardiomyocyte injury model.
- Our data showed that RBP4 upregulation in heart markedly promotes pyroptosis through an interaction with NLRP3 (nucleotide-binding oligomerization domain-like receptor family pyrin domain-containing 3) in the progression of acute myocardial infarction, while knockdown of RBP4 in heart decreased infarct size and protected against acute myocardial infarction-induced cardiac dysfunction in mice.

What Are the Clinical Implications?

- Our results indicating that lowering RBP4 levels might serve as a promising therapeutic approach for acute myocardial infarction prevention and treatment.

Nonstandard Abbreviations and Acronyms

| | |
|--------------|--|
| ASC | apoptosis-associated speck-like protein containing a caspase recruitment domain |
| GSDMD | gasdermin-D |
| I/H | ischemia-hypoxia |
| NLRP3 | nucleotide-binding oligomerization domain-like receptor family pyrin domain-containing 3 |
| PI | propidium iodide |
| RBP4 | retinol-binding protein 4 |

then triggers pyroptosis and the release of proinflammatory interleukin (IL)-1 β and IL-18.³ Recent studies have demonstrated the involvement of cell pyroptosis in response to various pathological stresses, especially in post-AMI myocardium.^{4,5} Inhibition of pyroptosis can ameliorate myocardial injury, reduce infarct size, and prevent cardiac dysfunction after AMI.^{6–8} However, the detailed molecular mechanisms underlying pyroptosis in cardiomyocytes remain to be elucidated.

RBP4 (retinol-binding protein 4) is an \approx 21-kDa protein that transports retinol (vitamin A) in circulation.⁹ RBP4 was first identified as an important adipokine that contributes to insulin resistance and type 2 diabetes.^{10,11} Emerging evidences have linked elevated

circulating RBP4 to cardiovascular diseases, including atherosclerosis and coronary artery disease.¹² Our previous study indicated that serum RBP4 was associated with increased risk for the presence and severity of coronary artery disease.¹³ Another clinical study showed that plasma RBP4 was elevated in patients with inflammatory cardiomyopathy, indicating a potential proinflammatory effect of RBP4 in the heart.¹⁴ Indeed, we previously demonstrated that RBP4 activated NLRP3 inflammasome and promoted inflammation through Toll-like receptor 4 (TLR4)/myeloid differentiation primary response gene 88 pathway in cardiomyocyte.¹⁵ In addition, RBP4 expression was increased in ischemic cardiac tissue in a swine model of metabolic syndrome.¹⁶ However, the effect of RBP4 on pyroptosis and its role in the development of AMI have not been established.

To elucidate the underlying mechanisms for the role of RBP4 in AMI, we first evaluated the change of cardiac RBP4 expression in AMI models both in vivo and in vitro. Next, we examined the effects of RBP4 gain or loss of function on cardiomyocyte pyroptosis under ischemic stress. Moreover, we used the primary neonatal mouse cardiomyocytes to investigate the molecular mechanisms of RBP4-induced pyroptosis. Our findings suggest cardiac RBP4 as a novel modulator promoting cardiomyocyte pyroptosis in AMI.

METHODS

The data, analytic methods, and study materials will be made available on request to other researchers for purposes of reproducing the results or replicating the procedure.

AMI Model

For left anterior descending coronary artery ligation-induced AMI model,¹⁷ C57BL/6 male mice of 6- to 8-weeks old were anesthetized with 1.5% to 2% isoflurane, intubated, and placed on a respirator. Briefly, the third intercostal space was exposed, and the thoracic cavity was penetrated. After dissection, left anterior descending coronary artery was ligated using an 8-0 polyester suture. Successful ligation was confirmed as immediate pallor of the left ventricle surface and weakened movement of myocardium. Sham-operated mice underwent the same surgical procedure without the left anterior descending ligation. Echocardiography was performed using the Vevo2100 imaging system (VisualSonics Inc, Canada) with a 30-MHz central frequency scan head. Tissues were harvested at day 1, day 3, and day 7 after the surgical procedure. All animal protocols were in accordance with the ethical standards laid down in the 1964 Declaration of Helsinki and

its later amendments and approved by the Institutional Animal Care and Use Committee of Nanjing Medical University (permit number: IACUC-1905027).

Adenovirus-Mediated Cardiac RBP4 Knockdown

To achieve cardiac knockdown of RBP4, cardiac adenoviral gene transfer was performed as previously described.¹⁸ Immediately after coronary artery ligation, 50 μL of adenovirus solution containing 1×10^9 plaque-forming units (pfu) of either Ad-shRBP4 or Ad-scramble RNA (Hanbio, Shanghai, China) was injected at 4 sites in the peri-infarct region known as the “high-risk area” using a 30-gauge needle (12.5 μL per site). The information of sequences is presented in Table S1.

Cell Culture and Treatment

Neonatal mouse ventricular cardiomyocytes were isolated from 1- to 3-day old mice as described previously.¹⁵ In brief, minced ventricular tissue was digested with 0.4 mg/mL type II collagenase (Worthington biochemical Corp, USA) and 0.6 mg/mL pancreatin (Sigma-Aldrich, USA) at 37 °C. The isolated cells were first pre-plated for 30 minutes at 37 °C to allow fibroblasts to adhere. The unadhered cells were collected and further purified on a discontinuous Percoll (GE Healthcare, USA) density gradient. The gradient consisted of a 40.5% Percoll layer over a layer of 58.5% Percoll. After centrifugation at 1500g for 40 minutes with no deceleration brake, the purified cardiomyocytes were collected and maintained in DMEM/F12 containing 10% fetal bovine serum, 5% horse serum, 100 U/mL penicillin, and 100 $\mu\text{g}/\text{mL}$ streptomycin (Gibco, USA). For the construction of ischemia-hypoxia (I/H) model, cells were first serum starved overnight and then cultured with sugar- and serum-free DMEM/F12 in hypoxic condition (1% O_2) for 6 hours. To overexpress or knockdown RBP4, cardiomyocytes were infected with adenovirus (Hanbio, China) carrying the expression sequence of RBP4 or shRBP4 for 48 hours. To inhibit NLRP3, cells were transfected with specific siRNAs (RiboBio, China) using Lipofectamine RNAiMAX (Thermo Fisher Scientific, USA) for 24 hours (Table S2) and NLRP3 inhibitor MCC950 (10 $\mu\text{mol}/\text{L}$) (Sigma-Aldrich, USA) for 24 hours. Cells infected with empty adenovirus or scramble RNA were served as controls for overexpress or knockdown experiment, respectively. The information of sequences is presented in Table S1.

Triphenyltetrazolium Chloride Staining

To evaluate the infarct size, the frozen heart was sectioned into 1.2-mm thick from the apex to base. The

slides were then incubated in 1% triphenyltetrazolium chloride (Solarbio, China) for 15 minutes at 37 °C and then digitally photographed. Viable myocardium was red, whereas the infarct area was white. The results were analyzed by using SigmaScan Pro 5.0 (Systat Software, USA).

Assessment of Oxidative Stress

The activity of glutathione peroxidase and superoxide dismutase as well as the content of reactive oxygen species and malondialdehyde in the myocardium and cell culture medium were measured spectrophotometrically with commercial assay kits (Nanjing Jiancheng Bioengineering Institute, China) according to manufacturer's instructions.

Retinol and Retinyl Ester Measurements

Heart and serum retinol and retinyl ester levels were examined by liquid chromatography mass spectrometry as previously described.¹⁹ Briefly, heart tissues were homogenized in ice-cold PBS with a motorized homogenizer (Thermo Fisher Scientific, USA). An aliquot of 150 μL heart homogenates or serum was treated with an equal volume of acetonitrile and vortexed vigorously. Then 900 μL of pre-cooled tert-butyl methyl ether was added and vortexed. After standing at -20 °C for 1 hour, the solution was centrifuged at 4 °C, 13 500g for 20 minutes. The supernatant was evaporated to dryness. The samples were re-suspended in 1 mL of methanol prior to injection. An aliquot was injected into a 5500 QTRAP liquid chromatography mass spectrometry/MS instrument with APCI ionization (Applied Biosystems, USA). The autosampler was cooled to 4 °C and samples were placed in the closed compartment only immediately prior to injection. Analytes were separated using the following gradient protocol (flow, 400 $\mu\text{L}/\text{min}$; gradient, 0–0.1 minutes, 10% A and 90% B; 1–5 minutes, 45% A and 55% B; 5–6 minutes, 60% A and 40% B; 6–7.7 minutes, 60% A and 40% B; 7.7–7.8 minutes, 10% A and 90% B; 7.8–10 minutes, 5% A and 95% B). Mobile phase A: 5% acetonitrile, 20 mmol/L ammonium acetate and mobile phase B: 100% acetonitrile. Quantification was performed by interpolation and linear least-squares regression using Skyline software (China).

Cell Viability Assay

To assess cell viability of cardiomyocytes, Cell Counting Kit-8 assays (Dojindo, Japan) were performed according to the manufacturer's instructions. Cardiomyocytes were cultured in a 96-well plate at a density of 1×10^4 cells/well. After treatment with I/H for 6 hours or adenovirus (Hanbio, China) carrying

the expression sequence of RBP4 or shRBP4 for 48 hours, 10 μ L of Cell Counting Kit-8 solution was added to each well, and further cultured at 37 °C for 1 hour. The absorbance was detected at the wavelength of 450 nm using a microplate reader (Synergy H1, BioTek, USA).

Hoechst 33342/Propidium Iodide Fluorescent Staining

Cell pyroptosis was detected by double staining with fluorescent dyes Hoechst 33342 (Sigma-Aldrich, USA) and propidium iodide (PI) (Sigma-Aldrich, USA) staining. Briefly, cardiomyocytes were cultured in 24-well plates, and then Hoechst 33342 and PI were added to the cultured medium at final concentrations of 1.5 and 8 mol/L, respectively. After incubation at 37 °C for 30 minutes, the stained cells were observed using a fluorescence microscope with Cellsens Dimention 1.15 software (Olympus, Japan). The total number of cells and the number of damaged cells were counted under $\times 200$ magnification in triplicate.

Lactate Dehydrogenase Release Assay

Cardiomyocytes culture supernatants or marginal tissue of heart infarction were collected, and the lactate dehydrogenase (LDH) activity was detected using the LDH assay kit (Nanjing Jiancheng Bioengineering Institute, China). Briefly, 20 μ L of cell supernatant and 25 μ L of substrate were mixed together and incubated at 37 °C for 15 minutes. Then 25 μ L 2,4-dinitrophenylhydrazine was added into the samples and incubated at 37 °C for 15 minutes. Finally, 250 μ L 0.4 mol/L NaOH solution was added and incubated at room temperature for 5 minutes. The absorbance was measured at 450 nm on a spectrophotometric microplate reader (Synergy H1, BioTek, USA).

Immunofluorescence Staining

Immunofluorescence staining on frozen heart sections or primary cardiomyocytes was performed as described previously.¹⁵ Briefly, after incubation with anti- α -actinin (1:200, Sigma-Aldrich, USA), anti-RBP4 (1:200, Abcam, UK), anti-F4/80 (1:50, Santa Cruz, USA), anti-NLRP3 (1:200, Cell Signaling, USA) or anti- α -SMA (1:200, Sigma-Aldrich, USA) overnight at 4 °C, Alexa Fluor 594-conjugated secondary antibody (1:200, Life Technology, USA) was added to visualize the staining. 4',6-diamidino-2-phenylindole (DAPI, 1 μ g/mL, Sigma, USA) was used to counterstain the nuclei. The staining was observed and quantified in 10 randomly selected areas of each sample using a fluorescence microscope with Cellsens Dimention 1.15 software (Olympus, Japan).

Serum RBP4, IL-1 β , and IL-18 Measurement

Serum RBP4 levels were determined by quantitative Western blotting¹⁵ using purified mouse RBP4 (Sino Biological, China) for generating the standard curves. Serum levels of IL-1 β and IL-18 were determined using the mouse ELISA Kits (Cusabio, China) according to the manufacturer's instructions.

Quantitative Real-Time Polymerase Chain Reaction

Total RNA was extracted by TRIzol Reagent (Invitrogen, USA) and reverse transcribed to cDNA using Reverse Transcription Master Kit (Toyobo, Japan) according to the manufacturer's instructions. Real-time polymerase chain reaction was performed on LightCycler@480 Instrument (Roche, Swiss) using SYBR Green I Master mix (Roche, Swiss). The relative gene expression levels were determined using the $2^{-\Delta\Delta CT}$ method using TBP (Tata-binding protein) as an internal control. The primer sequences are listed in Table S3.

Western Blot

Tissues or cells were lysed in radioimmunoprecipitation assay buffer containing 1 mmol/L NaF, 1 mmol/L sodium orthovanadate, and 1 mmol/L phenylmethylsulfonyl fluoride. Protein concentrations were measured by BCA assay (Beyotime Biotechnology, China). Equal amounts of protein were separated by 4% to 20% GenScript's SurePAGETM Bis-Tris gels (GenScript Biotechnology, China) and transferred to polyvinylidene fluoride membranes (Millipore, USA). The following primary antibodies were used: anti RBP4 (Abcam, ab109193, UK), anti-Caspase-1 (Abcam, ab179515, UK), anti-IL-18 (Abcam, ab71495, UK), anti-Tublin (Abcam, ab6046, UK), anti-GSDMD (L60) (Cell Signaling, #93709, USA), anti-NLRP3 (Cell Signaling, #15101, USA), anti-IL-1 β (Cell Signaling, #12242, USA), anti- β -actin (Cell Signaling, #4970, USA), anti-Cleaved GSDMD (Cell Signaling, #50928, USA), anti-ASC (Santa Cruz, sc-514414, USA). Chemiluminescence detection was performed after incubation with horseradish peroxidase-conjugated secondary antibody (GE Healthcare, USA) using the ChemiDocTM XRS+ System (Bio-Rad, USA). The intensity of immunoreactivity was assessed using Image Lab 6.0 software (Bio-Rad, USA).

Coimmunoprecipitation Assay

For analyzing the interaction between RBP4 and NLRP3, aliquots of equal protein were used for immunoprecipitation. The samples were incubated with rabbit polyclonal immunoglobulin G control antibody

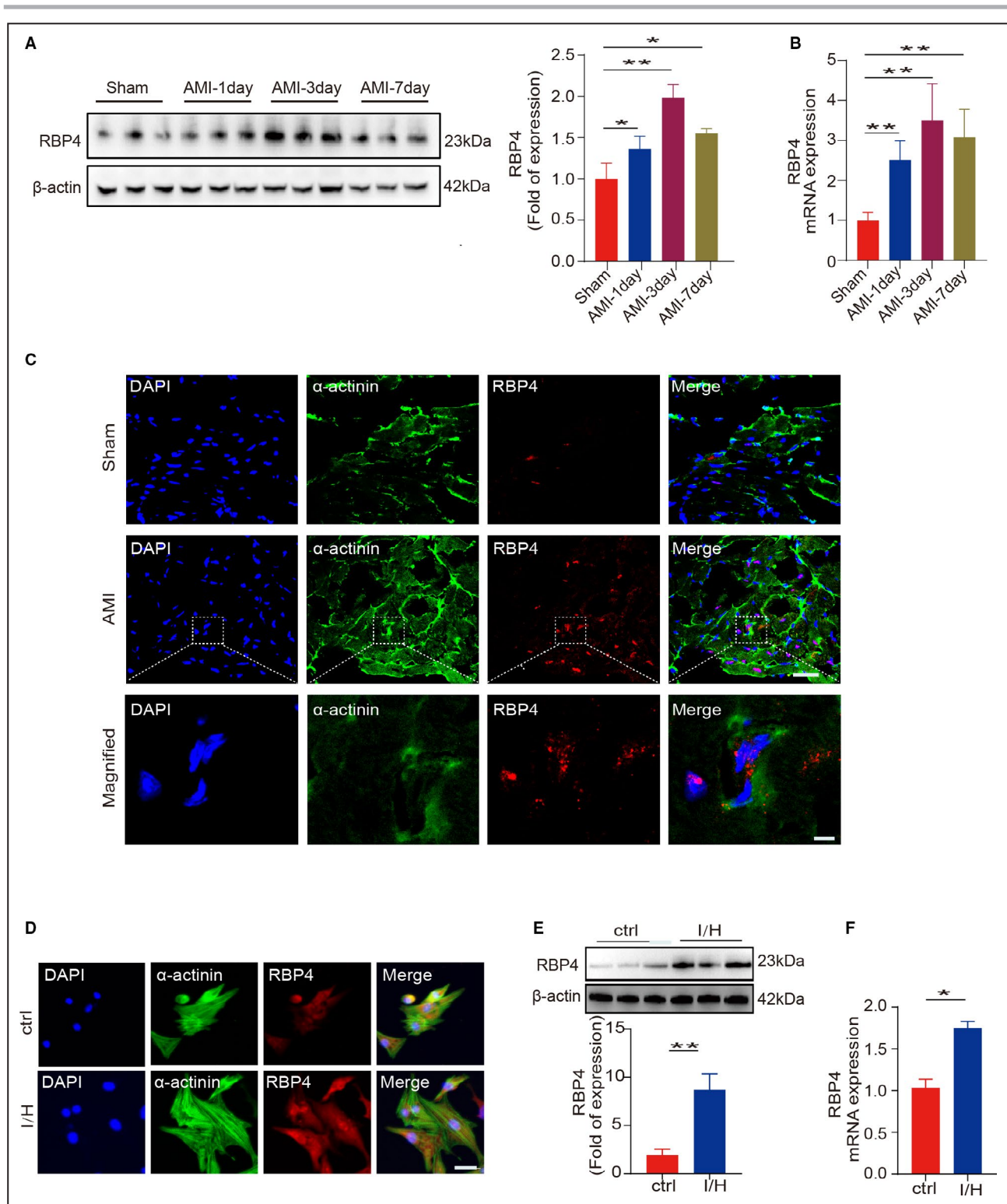


Figure 1. RBP4 (retinol-binding protein 4), expression is increased in acute myocardial infarction both in vivo and in vitro. **A** and **B**, RBP4 protein (**A**) and mRNA (**B**) levels in the border zone of infarct myocardium at day 1, day 3, and day 7 post-acute myocardial infarction and sham controls; $n=6$; $*P<0.05$ vs sham; $**P<0.01$ vs sham. **C**, Immunofluorescence staining of heart tissue sections with anti-RBP4 antibody (red), anti- α -actinin (green) and DAPI (blue). Scale bar=40 μ m. For the construction of ischemia-hypoxia model, primary cardiomyocytes were first serum starved overnight and then cultured with sugar- and serum-free DMEM/F12 in hypoxic condition (1% O_2) for 6 hours. **D**, Immunofluorescence staining of cardiomyocytes with anti-RBP4 antibody (red), anti- α -actinin (green) and 4',6-diamidino-2-phenylindole (blue). Scale bar=80 μ m. **E** and **F**, RBP4 protein (**E**) and mRNA (**F**) levels in cardiomyocytes treated with ischemia-hypoxia; $n=6$; $*P<0.05$ vs control; $**P<0.01$ vs control. AMI indicates acute myocardial infarction; DAPI, 4',6-diamidino-2-phenylindole; I/H, ischemia/hypoxia; and RBP4, retinol-binding protein 4.

(Cell Signaling, #2729, USA), anti-VeriBlot for immunoprecipitation detection (Abcam, ab131366, UK), anti-RBP4 or anti-NLRP3. After rotating for 4 hours at 4 °C, a total of 25 µL resuspended volume of protein G agarose beads were added and continued rotating for another 2 hours. The eluted proteins were then immunoblotted with the anti-RBP4 and anti-NLRP3.

Statistical Analysis

Data are presented as mean±SD unless otherwise specified. Statistical differences were assessed using unpaired Student 2-tailed *t*-tests for 2 groups and a 1-way ANOVA for ≥3 groups. Spearman correlation analysis was used for the correlations of cardiac RBP4 expression with serum pyroptosis-related markers. A *P* value of <0.05 was considered significant.

RESULTS

RBP4 Expression Is Increased in AMI Both In Vivo and In Vitro

To evaluate the possible involvement of RBP4 in the pathogenesis of AMI, we first examined RBP4 expression in the heart of AMI mice and I/H treated cardiomyocytes. AMI model was confirmed by echocardiography (Figure S1A and Table S4) and triphenyltetrazolium chloride staining (Figure S1B). Although RBP4 expression was lower in the heart when compared with the 2 identified major origins of RBP4, liver, and adipose tissue²⁰ (Figure S1F); however, remarkable elevation of RBP4 expression was detected in the border zone of infarct myocardium in mice (Figure 1A and 1B) as well as in I/H-treated cardiomyocytes (Figure 1E and 1F). By contrast, no significant changes of RBP4 expression were observed in serum, liver, white adipose tissue, and brown adipose tissue after AMI (Figure S1D and S1E). Immunofluorescent staining showed that RBP4 was increased in the myocardium of AMI mice and I/H-treated cardiomyocytes that were positive for the cardiomyocyte marker α -actinin (Figure 1C and 1D).

Taken together, these data suggest that RBP4 is selectively upregulated in the ischemic heart in AMI.

Knockdown of RBP4 Attenuates I/H-Induced Cardiomyocyte Injury

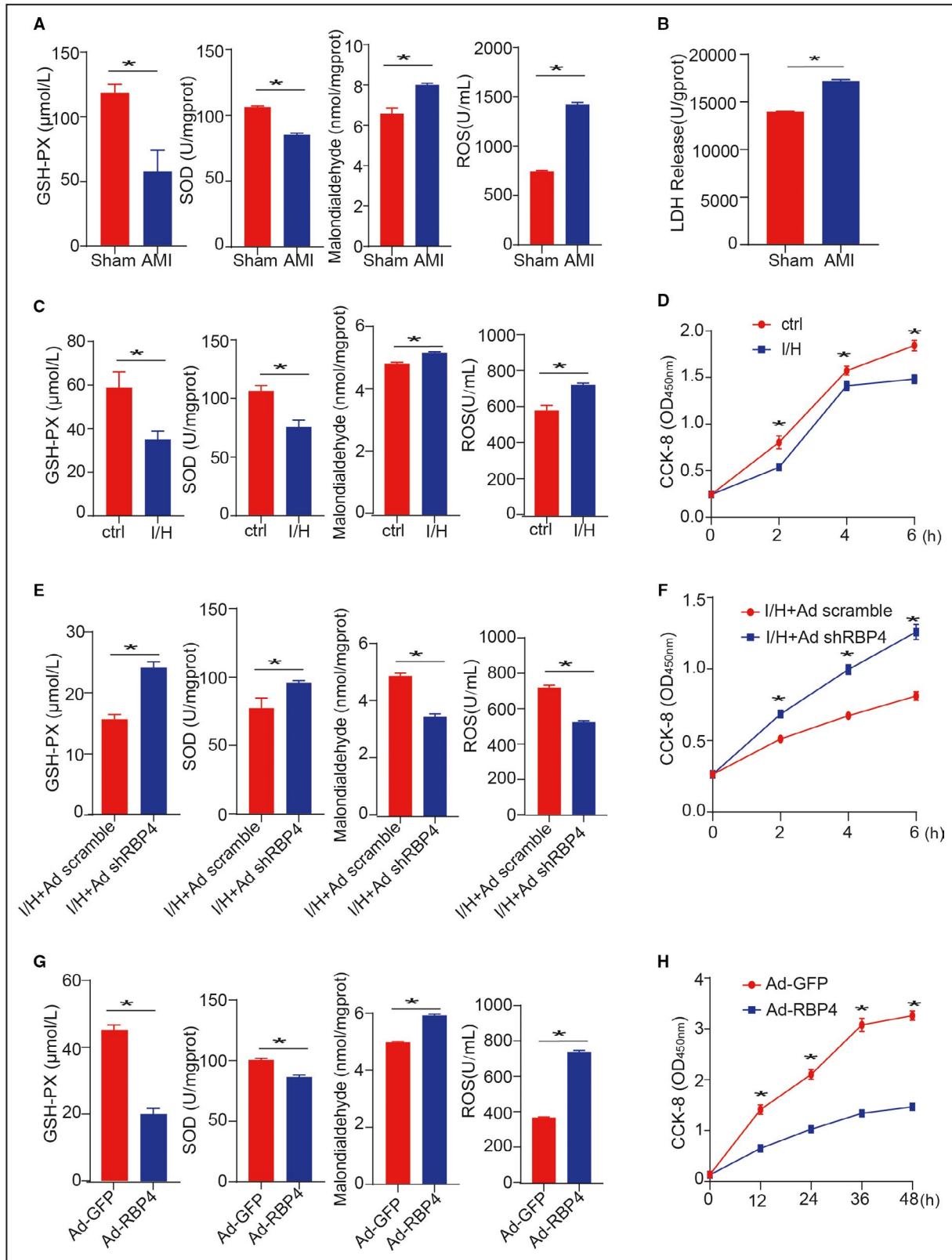
Oxidative stress was induced in the myocardium of AMI mice as evidenced by decreased glutathione peroxidase and superoxide dismutase as well as increased malondialdehyde and reactive oxygen species (Figure 2A). Moreover, an increase of LDH release was also detected in the hearts of AMI mice (Figure 2B), indicating cardiac injury. To further investigate the effects of RBP4 in I/H-induced cardiomyocyte injury, oxidative stress, and cell viability were measured. After I/H treatment for 6 hours, levels of glutathione peroxidase and superoxide dismutase were decreased while malondialdehyde and reactive oxygen species were increased in cardiomyocytes, indicating increased oxidative stress (Figure 2C). Cell Counting Kit-8 assay showed that I/H-treated cardiomyocytes had lower viability in comparison with the control cardiomyocytes (Figure 2D). Knockdown of RBP4 alleviated oxidative stress (Figure 2E) and increased the cell viability (Figure 2F) in I/H-treated cardiomyocytes. By contrast, overexpression of RBP4 promoted oxidative stress (Figure 2G) and impaired cell viability (Figure 2H) in cardiomyocytes.

Upregulation of RBP4 Is Positively Correlated With Pyroptosis-Related Markers in AMI

Given that RBP4 has been considered as a proinflammatory factor,²⁰ we then investigated the association of cardiac RBP4 expression with pyroptosis-related markers in AMI mice. Pyroptosis was activated in the border zone of infarct myocardium as evidenced by greater NLRP3 inflammasome activation, increased cleavage of Caspase-1 and GSDMD, as well as upregulated IL-1 β and IL-18 (Figure 3A). Consistently, mRNA levels of NLRP3, ASC (apoptosis-associated speck-like protein containing a caspase recruitment domain), Caspase-1, GSDMD, IL-1 β and IL-18 were increased

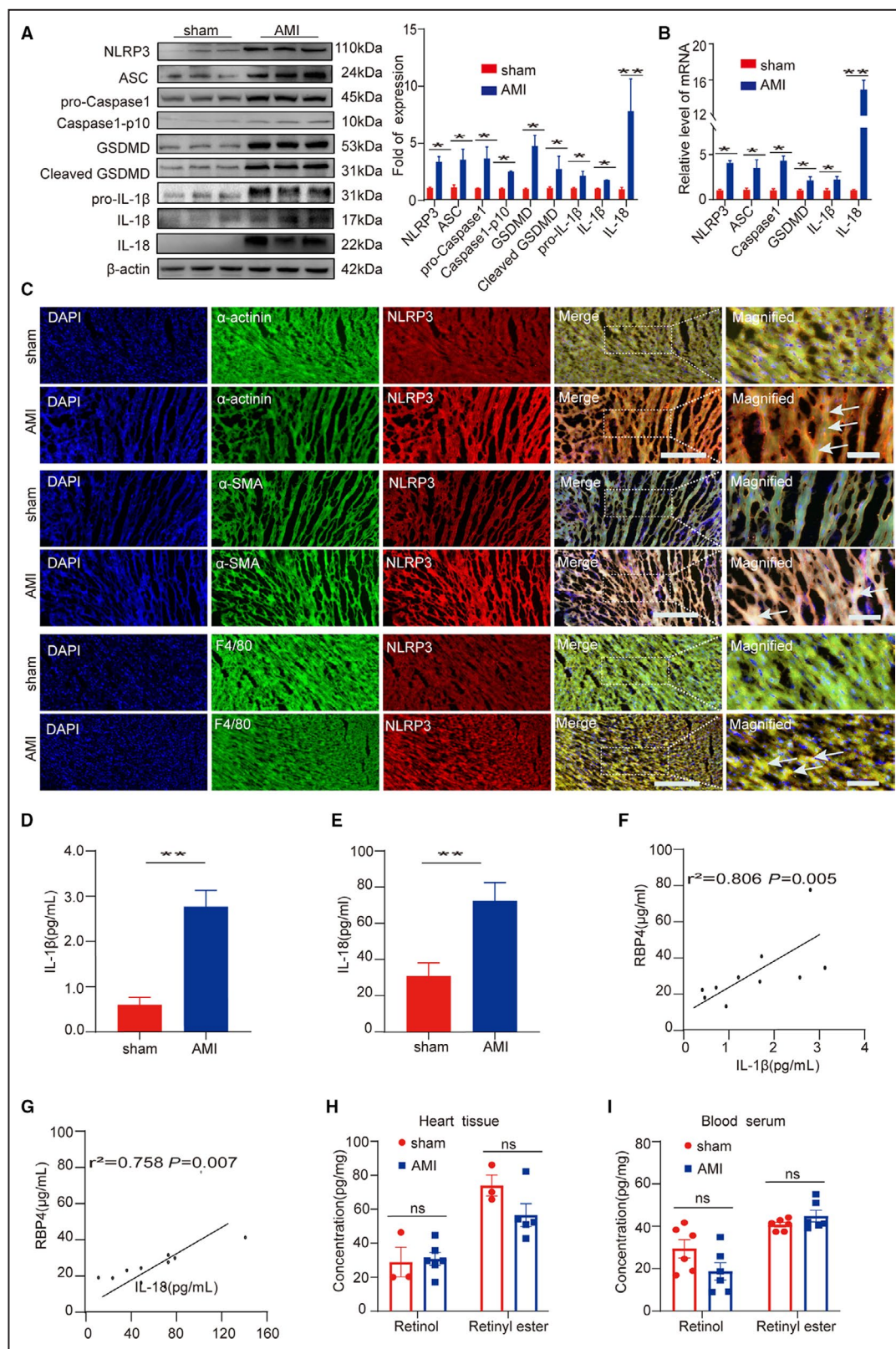
Figure 2. RBP4 (retinol-binding protein 4), regulates ischemia-hypoxia-induced oxidative stress and cell injury in cardiomyocytes.

A, The indexes of oxidative stress including glutathione peroxidase, superoxide dismutase, malondialdehyde, and reactive oxygen species were measured at day-3 post-acute myocardial infarction and sham controls. **B**, Lactate dehydrogenase release in the myocardium at day-3 post-acute myocardial infarction and sham controls; n=6; **P*<0.05 vs sham. **C** and **D**, Primary cardiomyocytes were treated with ischemia-hypoxia for 6 hours. The indexes of oxidative stress including glutathione peroxidase, superoxide dismutase, malondialdehyde, and reactive oxygen species (**C**) as well as the cell viability (**D**) were measured; n=6; **P*<0.05 vs control. **E** and **F**, Primary cardiomyocytes were transfected with adenovirus carrying shRBP4 or scramble RNA for 48 hours and then treated with ischemia-hypoxia for 6 hours. The indexes of oxidative stress (**E**) and cell viability (**F**) were measured; n=6; **P*<0.05 vs ischemia-hypoxia+Ad scramble. **G** and **H**, Primary cardiomyocytes were transfected with adenovirus carrying the expression sequence of RBP4 or GFP for 48 hours. The indexes of oxidative stress (**G**) and cell viability (**H**) were measured; n=6; **P*<0.05 vs Ad-GFP. AMI indicates acute myocardial infarction; CCK-8, Cell Counting Kit-8; GFP, green fluorescent protein; GSH-PX, glutathione peroxidase; I/H, ischemia/hypoxia; RBP4, retinol-binding protein 4; ROS, reactive oxygen species; and SOD, superoxide dismutase.



in AMI mice (Figure 3B). Immunofluorescent staining showed that NLRP3 was dramatically activated not only in cardiomyocytes, but also in macrophages

and fibroblasts (Figure 3C). Importantly, serum levels of IL-1 β and IL-18 were significantly elevated in AMI mice compared with sham controls (Figure 3D



and 3E). Quantitative level of cardiac RBP4 expression was calculated using purified mouse RBP4 for generating the standard curves (Figure S1C) as

previously described.¹⁰ Spearman correlation analyses showed that cardiac RBP4 expression levels were positively correlated with serum levels of IL-1β and

Figure 3. RBP4 (retinol-binding protein 4), expression is correlated with cardiac proptosis in acute myocardial infarction.

A and B, The expression levels of NLRP3 (nucleotide-binding oligomerization domain-like receptor family pyrin domain-containing 3) inflammasome and pyroptosis-related genes in the myocardium of acute myocardial infarction mice and sham controls were examined western blot (**A**) and quantitative real-time polymerase chain reaction (**B**); $n=6$; $*P<0.05$ vs sham; $**P<0.01$ vs sham. **C**, Immunofluorescence staining of heart tissue sections with anti-NLRP antibody (red) and 4',6-diamidino-2-phenylindole (blue) together with cell-specific marker (green), including anti- α -actinin (cardiomyocyte), anti-F4/80 (macrophage), and anti- α -SMA (fibroblast). Scale bar=40 μ m. Arrows represent double positive cells. **D and E**, Serum interleukin-1 β (**D**) and interleukin-18 (**E**) levels in acute myocardial infarction mice and sham controls. $**P<0.01$ vs sham; $n=6$ per group. **F and G**, Cardiac RBP4 protein concentrations are positively correlated with serum interleukin-1 β (**F**) and interleukin-18 (**G**). **H and I**, Retinol and retinyl ester levels in the heart (**H**) and serum (**I**) in acute myocardial infarction mice and sham controls. ns indicates no significance; $n=6$ per group. AMI indicates acute myocardial infarction; ASC, apoptosis-associated speck-like protein containing a caspase recruitment domain; DAPI, 4',6-diamidino-2-phenylindole; GSDMD, gasdermin-D; I/H, ischemia/hypoxia; IL-1 β , interleukin-1 β ; IL-18, interleukin-18; NLRP3, nucleotide-binding oligomerization domain-like receptor family pyrin domain-containing 3; and RBP4, retinol-binding protein 4.

IL-18 (Figure 3F and 3G), indicating that upregulated RBP4 may be associated with the activation of cardiomyocyte pyroptosis in AMI. By contrast, no significant changes in the levels of retinol and retinyl ester were observed either in the heart or in the serum of AMI mice, when compared with those in the sham-operated mice (Figure 3H and 3I).

RBP4 Regulates Cardiomyocyte Pyroptosis

We then investigated the effects of RBP4 on I/H-induced pyroptosis in cardiomyocytes. After I/H treatment, there were intense NLRP3 inflammasome activation and cleavage of Caspase-1 and GSDMD in cardiomyocytes (Figure 4A). Since cardiomyocyte per se cannot secrete IL-1 β ,²¹ we only detected increased protein level of IL-18 (Figure 4A). Similar results were observed at the mRNA levels of NLRP3, ASC, Caspase-1, GSDMD, and IL-18 in I/H-treated cardiomyocytes (Figure 4B). Moreover, the percentage of propidium iodide-positive staining cells (Figure 4C) and LDH activity (Figure 4D) were increased also in I/H-treated cardiomyocytes, indicating activated pyroptosis by I/H stimulation. Knockdown of RBP4 by infection with adenovirus carrying shRBP4 (Figure 4E) significantly attenuated I/H-induced pyroptosis, as indicated by reduced activation of NLRP3 inflammasome and cleavage of Caspase-1 and GSDMD, as well as decreased expression of IL-18 (Figure 4F). Consistently, knockdown of RBP4 also decrease the percentage of PI-positive staining cells (Figure 4G) and LDH activity (Figure 4H) in I/H-treated cardiomyocytes. By contrast, overexpression of RBP4 in cardiomyocytes (Figure 4I) triggered the activation of NLRP3 inflammasome, promoted the cleavage of Caspase-1 and GSDMD (Figure 4J), increased the percentage of PI-positive staining cells (Figure 4K), and LDH activity (Figure 4L). Taken together, these data suggest that upregulation of RBP4 can induce pyroptosis in cardiomyocytes.

RBP4 Regulates Cardiomyocyte Pyroptosis Via Interaction With NLRP3

Activation of NLRP3 inflammasome is an important mechanism for pyroptosis.³ To investigate whether NLRP3 was involved in the RBP4-induced cardiomyocyte pyroptosis, the potential association between RBP4 and NLRP3 proteins in cardiomyocytes was assessed by coimmunoprecipitation followed by immunoblotting. As shown in Figure 5A, RBP4 and NLRP3 were enriched either in the immunoprecipitation: NLRP3 or immunoprecipitation: RBP4 samples, as evidenced by the prominent bands corresponding to RBP4 and NLRP3 proteins, confirming a protein interaction between RBP4 and NLRP3. Notably, knockdown of NLRP3 (Figure S2) attenuated RBP4-induced cardiomyocyte pyroptosis, as evidenced by decreased expression levels of ASC, pro-Caspase-1, Caspase-1-p10, GSDMD, cleaved GSDMD, and IL-18 (Figure 5B). The percentage of PI-positive staining cells (Figure 5C) and LDH activity (Figure 5D) were also suppressed by NLRP3 siRNA. Similar results were observed in RBP4 overexpressed cardiomyocytes treated with NLRP3 specific inhibitor MCC950 (Figure 5E through 5G). Collectively, these data suggest that RBP4 activates cardiomyocyte pyroptosis through an interaction with NLRP3.

Knockdown of RBP4 in Heart Attenuates Cardiac Pyroptosis in AMI

We next determined whether RBP4 is required for the induction of cardiac pyroptosis in AMI. Adenovirus carrying shRBP4 was delivered to the myocardium by intrapericardial injection. As shown in Figure 6A, RBP4 was specifically knockdown in heart, but not in liver and adipose tissue. Consistent with the results of in vitro experiments, AMI-induced activation of NLRP3 inflammasome, cleavage of Caspase-1 and GSDMD, increased expression of IL-1 β , IL-18, and LDH activity were significantly inhibited by the knockdown of RBP4 (Figure 6B and 6C). These findings support that knockdown of RBP4 could attenuate NLRP3-mediated pyroptosis in AMI.

Knockdown of RBP4 in Heart Protects Against Cardiac Dysfunction After AMI

We then asked whether inhibition of RBP4 might be beneficial to the cardiac function after AMI.

Triphenyltetrazolium chloride staining showed that knockdown of RBP4 in heart significantly decreased the infarct size at day 3 after the ligation of left anterior descending (Figure 6D). In addition, the expression

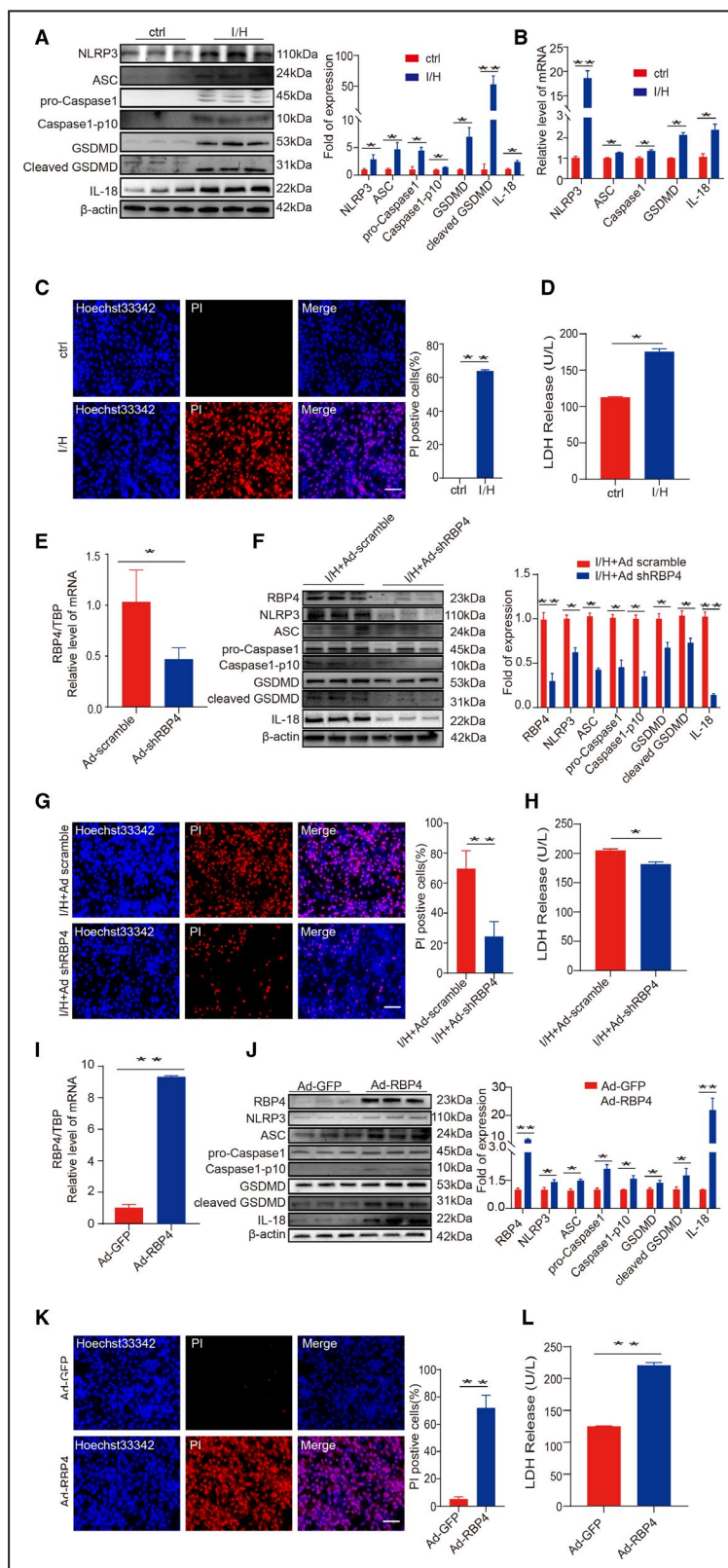


Figure 4. RBP4 (retinol-binding protein 4) regulates pyroptosis in cardiomyocytes.

A and B, The protein (**A**) and mRNA (**B**) levels of NLRP3 (nucleotide-binding oligomerization domain-like receptor family pyrin domain-containing 3) inflammasome and pyroptosis-related genes in cardiomyocytes treated with ischemia-hypoxia for 6 hours; n=6; * $P<0.05$ vs ctrl; ** $P<0.01$ vs ctrl. **C**, The percentage of propidium iodide (red) positive cells after ischemia-hypoxia treatment for 6 hours. ** $P<0.01$ vs ctrl. **D**, Lactate dehydrogenase release in cardiomyocytes treated with ischemia-hypoxia for 6 hours. * $P<0.05$ vs ctrl. **E through H**, Primary cardiomyocytes were transfected with adenovirus carrying shRBP4 or scramble RNA for 48 hours and then treated with ischemia-hypoxia for 6 hours. Protein levels of NLRP3 inflammasome and pyroptosis-related genes were detected by western blot (**F**). The percentage of propidium iodide (red) positive cells (**G**) and Lactate dehydrogenase release (**H**) were reduced by knockdown of RBP4; n=6; * $P<0.05$ vs scramble; ** $P<0.01$ vs scramble. **I through L**, Primary cardiomyocytes were transfected with adenovirus carrying the expression sequence of RBP4 or GFP for 48 hours. Protein levels of NLRP3 inflammasome and pyroptosis-related genes were detected by western blot (**J**). The percentage of propidium iodide (red) positive cells (**K**) and lactate dehydrogenase release (**L**) were increased by overexpression of RBP4; n=6; * $P<0.05$ vs GFP; ** $P<0.01$ vs GFP. AMI indicates acute myocardial infarction; ASC, apoptosis-associated speck-like protein containing a caspase recruitment domain; GFP, green fluorescent protein; GSDMD, gasdermin-D; I/H, ischemia/hypoxia; IL-1 β , interleukin-1 β ; IL-18, interleukin-18; LDH, lactate dehydrogenase; NLRP3, nucleotide-binding oligomerization domain-like receptor family pyrin domain-containing 3; PI, propidium iodide; and RBP4, retinol-binding protein 4.

levels of hypertrophic markers, including atrial natriuretic peptide, brain natriuretic peptide, and myosin heavy chain 7, were decreased in the left ventricular myocardium of RBP4 knockdown mice (Figure 6E). Echocardiography demonstrated that the left ventricular internal dimension and left ventricular volume were also decreased by inhibition of RBP4 (Figure 6F and Table S5), indicating attenuated adverse cardiac remodeling. Importantly, knockdown of RBP4 significantly improved AMI-induced decrease of left ventricular ejection fraction and fractional shortening (Figure 6F). The results indicate that silencing RBP4 could protect against cardiac dysfunction after AMI.

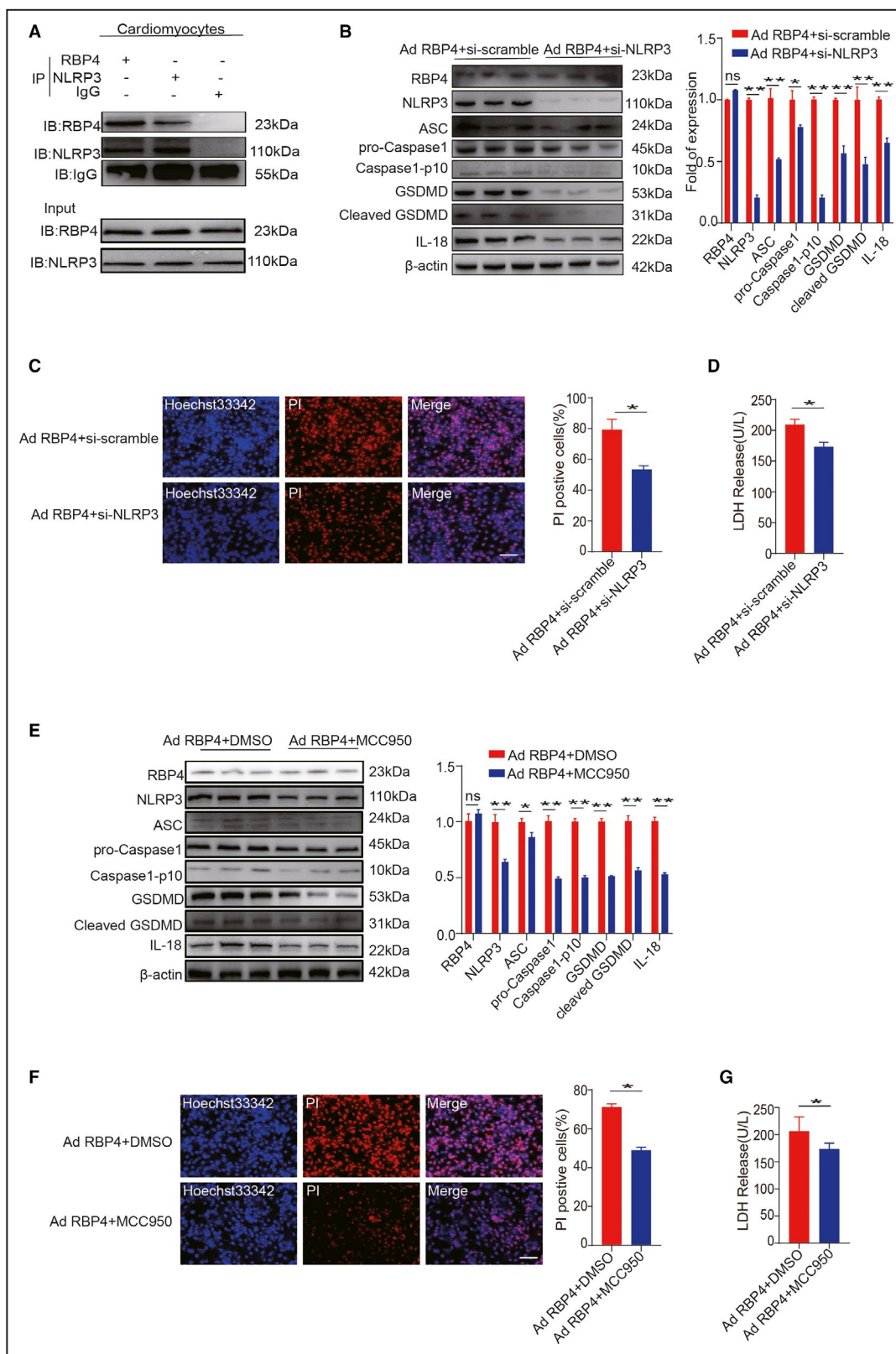
DISCUSSION

Our present study provides novel evidence indicating that RBP4 upregulation in heart markedly promotes pyroptosis through an interaction with NLRP3 in the progression of AMI. We first demonstrated that RBP4 was increased both in the myocardium of AMI mice and I/H-treated cardiomyocytes. The results of in vitro and in vivo experiments further demonstrated that elevated RBP4 exacerbated cardiomyocytes pyroptosis through its direct interaction of NLRP3 in AMI. Finally, knockdown of RBP4 in heart decreased infarct size and protected against AMI-induced cardiac dysfunction in mice. Thus, lowering RBP4 levels might serve as a promising therapeutic approach for AMI prevention and treatment.

Increasing numbers of human studies have indicated the association of circulating RBP4 as an insulin-resistant adipokine that contributes to the risk of cardiovascular diseases¹²; however, controversial results are observed in patients with AMI. Pan et al²² found that plasma RBP4 levels were significantly lower in patients with ST-segment-elevation AMI quantified by both isobaric tags for relative and absolute quantitation and ELISA, which was consistent with the results of the other 2 studies.^{23,24} By contrast, Lambadiari et al²⁵ reported that serum RBP4 levels were increased in patients with AMI. Although the reasons for the

discrepancies may relate to multiple factors, such as different study populations, sample size, and assay methods,²⁶ neither the causal effect nor the protective value of RBP4 levels in AMI have been confirmed. We here showed that RBP4 was upregulated in the myocardium of AMI mice despite no changes of RBP4 levels in its 2 primary sources, liver, and adipose tissue.²⁰ Knockdown of RBP4 in heart protected against adverse cardiac remodeling and cardiac dysfunction after AMI. Importantly, our study also provides the first experimental evidence that RBP4 upregulation exacerbated whereas RBP4 downregulation attenuated I/H-induced cardiomyocyte injury. However, to better delineate its causal role in AMI, future studies in cardiac-specific RBP4 knockout mice are still needed.

The upregulated RBP4 in the myocardium of AMI mice may originate from cardiomyocytes per se, which is supported by the colocalization of RBP4 and cardiomyocyte-specific marker α -actinin both in vivo and in vitro. Moreover, both the mRNA and protein levels of RBP4 was increased in I/H-treated cardiomyocytes. To date, the precise molecules and exact mechanism regulating RBP4 synthesis remain to be further elucidated. RBP4 levels are primarily regulated by the availability of retinol in the liver, where retinol binding promotes the secretion of RBP4 into circulation from hepatocytes.²⁷ Accumulation of retinol in infarcted hearts has been reported in mice model of AMI,¹⁹ indicating a potential mechanism by which increased retinol binds recruits more RBP4 in the ischemic myocardium. However, retinol levels were similar both in the hearts and serum of AMI and sham-operated mice in our study. This discrepancy may be because the differences in the region of detected heart. In their study, increased level of retinol was only found in the infarcted region but not in the peri-infarct zone,¹⁹ the latter of which is consistent with our results. A recent study demonstrated that activation of the kinase mechanistic target of rapamycin in complex 1 dramatically enhanced RBP4 mRNA translation in hepatocytes.²⁸ Intriguingly, cardiac mechanistic target of rapamycin in complex 1 is also activated and plays a crucial role



in the pathological cardiac remodeling in myocardial ischemia,²⁹ which may contribute to the upregulated cardiac RBP4 expression in AMI. Deng et al³⁰ reported

that adipose tissue can release RBP4-rich exosome-like vesicles which are taken up by peripheral blood monocytes. Although no significant change of serum

Figure 5. RBP4 (retinol-binding protein 4) regulates cardiomyocyte pyroptosis via interacting with NLRP3 (nucleotide-binding oligomerization domain-like receptor family pyrin domain-containing 3).

A, Co-immunoprecipitation identified a protein interaction between RBP4 and NLRP3 in primary cardiomyocytes. **B** through **D**, Primary cardiomyocytes were transfected with adenovirus carrying the expression sequence of RBP4 for 24 hours, and then transfected with NLRP3 siRNA or scramble for 24 hours. Protein levels of RBP4, NLRP3 inflammasome and pyroptosis-related genes were detected by western blot (**B**). The percentage of propidium iodide (red) positive cells (**C**) and lactate dehydrogenase release (**D**) were reduced by silencing of NLRP3; $n=6$; $*P<0.05$ vs scramble; $**P<0.01$ vs scramble. **E** through **G**, Primary cardiomyocytes were transfected with adenovirus carrying the expression sequence of RBP4 for 24 hours, and then treated with NLRP3 inhibitor MCC950 (10 $\mu\text{mol/L}$) for 24 hours. Protein levels of RBP4, NLRP3 inflammasome and pyroptosis-related genes were detected by western blot (**E**). The percentage of propidium iodide (red) positive cells (**F**) and lactate dehydrogenase release (**G**) were reduced by inhibition of NLRP3; $n=6$; $*P<0.05$ vs DMSO; $**P<0.01$ vs DMSO. AMI indicates acute myocardial infarction; ASC, apoptosis-associated speck-like protein containing a caspase recruitment domain; GSDMD, gasdermin-D; IB, immunoblotting; I/H, ischemia/hypoxia; IgG, immunoglobulin G; IL-1 β , interleukin-1 β ; IL-18, interleukin-18; LDH, lactate dehydrogenase; NLRP3, nucleotide-binding oligomerization domain-like receptor family pyrin domain-containing 3; PI, propidium iodide; and RBP4, retinol-binding protein 4.

RBP4 level was observed in AMI mice in our experiments, further studies are still needed to investigate whether upregulated cardiac RBP4 is mediated by the intercellular cross-talk between hepatocytes/adipocytes and cardiomyocytes via exosomes.

RBP4-induced inflammation may be a common mechanism for its role in AMI since the expression of RBP4 was positively correlated with serum levels of proinflammatory factors IL-1 β and IL-18 in AMI mice. Pyroptosis is a proinflammatory programmed cell death

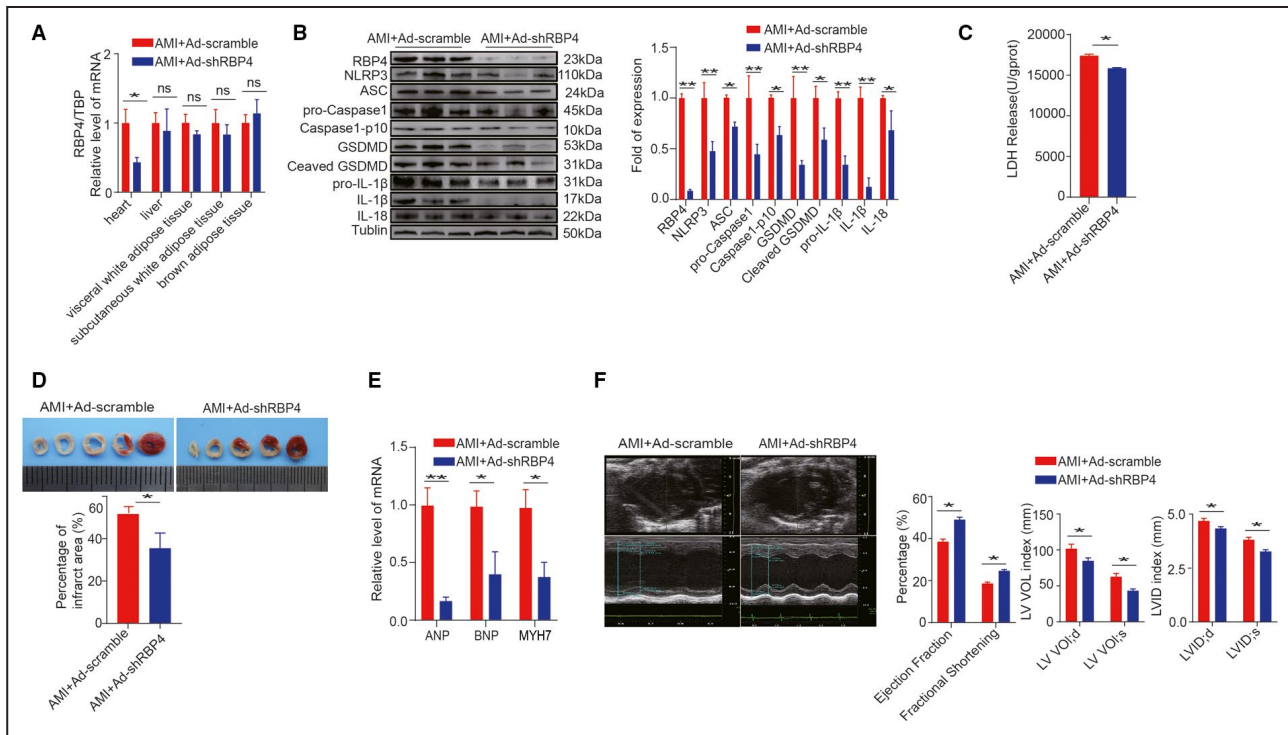


Figure 6. Knockdown of RBP4 (retinol-binding protein 4) in heart attenuates cardiac pyroptosis and cardiac dysfunction in acute myocardial infarction.

Adenovirus carrying shRBP4 was delivery to the myocardium by intrapericardial injection immediately after the ligation of left anterior descending. **A**, RBP4 mRNA level was detected in different tissues. **B**, Protein levels of RBP4, NLRP3 (nucleotide-binding oligomerization domain-like receptor family pyrin domain-containing 3) inflammasome, and pyroptosis-related genes were detected by Western blot. **C**, Lactate dehydrogenase release in the left ventricular myocardium. **D**, Triphenyltetrazolium chloride staining of infarct size at day 3 after the ligation of left anterior descending. **E**, mRNA levels of atrial natriuretic peptide, brain natriuretic peptide, and myosin heavy chain 7 in the left ventricular myocardium. **F**, Echocardiography data including left ventricular ejection fraction, fractional shortening, left ventricular volume, and left ventricular internal dimension; $n=5$; $*P<0.05$ vs scramble; $**P<0.01$ vs scramble. AMI indicates acute myocardial infarction; ANP, atrial natriuretic peptide; ASC, apoptosis-associated speck-like protein containing a caspase recruitment domain; BNP, brain natriuretic peptide; GSDMD, gasdermin-D; I/H, ischemia/hypoxia; IL-1 β , interleukin-1 β ; IL-18, interleukin-18; LV, VOL; d, left ventricular volume at end-diastole; LV, VOL; s, left ventricular volume at end-systole; LVID; d, left ventricular internal diameter at end-diastole; LVID; s, left ventricular internal diameter at end-systole; LDH, lactate dehydrogenase; MYH7, myosin heavy chain 7; NLRP3, nucleotide-binding oligomerization domain-like receptor family pyrin domain-containing 3; PI, propidium iodide; and RBP4, retinol-binding protein 4.

characterized by the cleavage of GSDMD to generate an N-terminal fragment, which oligomerizes to form cytotoxic pores in the cell membrane and consequent release of IL-1 β and IL-18.² The participation of pyroptosis in the process of AMI has been supported by animal studies.^{5,31} In cardiomyocytes, upregulation of RBP4 promoted the precursor cleavage of Caspase-1 and subsequently induced GSDMD-dependent pyroptosis. The results are consistent with our previous work showing that RBP4 treatment induced proinflammatory cytokine production and promotes cardiac hypertrophy.¹⁵ Furthermore, silencing of RBP4 in cardiomyocyte attenuated AMI-induced pyroptosis both in vitro and in vivo, indicating that upregulation of RBP4 may play a crucial role in the pathogenesis of AMI via activating pyroptosis. These findings indicate that RBP4 might function as a previously unrecognized proinflammatory myocardial factor in the progression of AMI.

The inflammatory response that occurs after AMI involves not only cardiomyocytes but also multiple types of other cells, including endothelial cells, fibroblasts, immune cells, etc.³² Exogenous RBP4 can activate macrophages and induce the secretion of proinflammatory cytokines, which in turn promotes insulin resistance in adipocytes.^{33,34} Moreover, overexpression of RBP4 in mice resulted in proinflammatory CD4 T-cell proliferation and Th1 polarization.^{35,36} The proinflammatory effect of RBP4 was also demonstrated in human endothelial

cells and suggested to contribute to cardiovascular diseases.³⁷ Therefore, RBP4 may promote cardiac inflammation via an autocrine/paracrine regulatory mechanism during the process of AMI. The protection of RBP4 knockdown against AMI-induced cardiac injury might also be mediated through inhibiting its proinflammatory effects in those non-cardiomyocyte cells. Further studies in cardiomyocyte-specific RBP4 knockout animals are required to assess more precisely the contribution of RBP4-induced cardiomyocyte inflammation to overall cardiac dysfunction after AMI.

Since the primary physiological function of RBP4 is to deliver retinol from liver to target tissues and retinol/retinoids have been implicated in the therapeutic strategy for the treatment of AMI,³⁸ the proinflammatory effect of RBP4 in cardiomyocytes could be retinol-dependent. However, no significant changes in retinol and retinyl ester levels were observed either in the hearts of AMI mice in our study or in the hearts of RBP4 knockout mice.³⁹ Therefore, RBP4 might induce cardiac inflammation through a retinol-independent mechanism. NLRP3 inflammasome plays a crucial role in the canonical pathway of pyroptotic cell death via cleaving and activating Caspase-1.⁴⁰ NLRP3 inflammasome is activated in cardiomyocytes during the infarct process, causing additional loss of functional myocardium.⁴¹ Inhibition of the NLRP3 in heart reduces inflammatory responses and infarct size, supporting the role of NLRP3 inflammasome in exacerbating the damage after AMI.⁴¹⁻⁴⁵ It is worth noting that the inflammatory

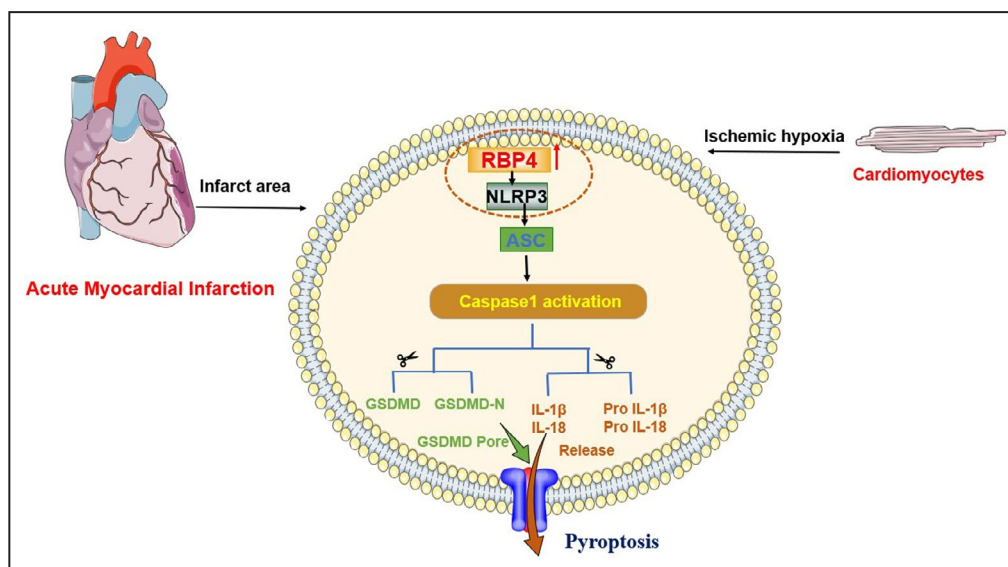


Figure 7. Potential role of RBP4 (retinol-binding protein 4) in acute myocardial infarction.

In the process of acute myocardial infarction, RBP4 is upregulated in ischemic cardiomyocytes. RBP4 directly binds to and activates NLRP3 (nucleotide-binding oligomerization domain-like receptor family pyrin domain-containing 3), which in turn induces Caspase-1 mediated cardiomyocyte pyroptosis. AMI indicates acute myocardial infarction; ASC, apoptosis-associated speck-like protein containing a caspase recruitment domain; GSDMD, gasdermin-D; IL-1 β , interleukin-1 β ; IL-18, interleukin-18; LDH, lactate dehydrogenase; NLRP3, nucleotide-binding oligomerization domain-like receptor family pyrin domain-containing 3; and RBP4, retinol-binding protein 4.

responses mediated by NLRP3 inflammasome activation depend on the cell type in which NLRP3 is activated.⁴⁶ In damaged myocardium, NLRP3 inflammasome contributes to pyroptosis and releasing of IL-18 and IL-1 β in cardiac fibroblasts^{47,48} and endothelial cells,⁴⁹ whereas it only contributes to pyroptosis and releasing of IL-18, but not IL-1 β , in cardiomyocytes.^{21,41,47} Consistently, we also could only detect the changes of NLRP3-mediated pyroptosis and IL-18 expression in our in vitro experiments. Importantly, NLRP3 inflammasome was activated in RBP4-overexpressed cardiomyocytes, whereas silencing of NLRP3 using either genetic or pharmacological inhibition suppressed RBP4-induced cardiomyocyte pyroptosis. These data collectively indicate that the NLRP3 inflammasome signaling was responsible for the inductive effects of RBP4 on pyroptosis in cardiomyocytes.

NLRP3 can be regulated by a wealth of different triggers such as K⁺ efflux, reactive oxygen species, autophagy, and mitochondrial dysfunction.⁴⁰ Several Toll-like receptors (TLRs) are activated after AMI, and their function is important for the priming and triggering of NLRP3 inflammasome.⁵⁰ We previously demonstrated that exogenous RBP4 activates NLRP3 inflammasome through TLR4-dependent pathway in cardiomyocytes.¹⁵ A recent study showed that RBP4 can act as an endogenous NLRP3-inflammasome priming agent through TLR2 and TLR4/MD2 in macrophage.³⁴ We now provide a novel mechanistic explanation for the activation of NLRP3 in AMI that RBP4 forms a complex with NLRP3 in cardiomyocytes. However, additional in-depth investigation is required to elucidate the precise mechanism governing the interaction between RBP4 and NLRP3 as well as the modulation of RBP4 on another component of NLRP3 inflammasome, ASC.

In summary, our data reveal that RBP4 plays a previously unrecognized pathological role in cardiomyocyte pyroptosis by an interaction with NLRP3 under ischemic condition (summarized in Figure 7). Our findings shed new light on the role of RBP4 in the progression of AMI. These findings suggest that cardiomyocyte RBP4 may represent a viable target for the management of cardiac dysfunction in patients with AMI.

ARTICLE INFORMATION

Received April 13, 2021; accepted September 24, 2021.

Affiliations

Department of Geriatrics, Sir Run Run Hospital (K.-Z.Z., X.-Y.S., M.W., L.W., H.-X.S., C.Z., J.-L.L., X.L., W.G.) and Key Laboratory for Aging and Disease (K.-Z.Z., X.-Y.S., M.W., L.W., H.-X.S., X.-Z.L., J.-J.H., X.-Q.L., C.W., C.Z., J.-L.L., X.L., W.G.) Nanjing Medical University, Nanjing, China and Department of Geriatrics, The Second Affiliated Hospital of Nanjing Medical University, Nanjing, China (K.-Z.Z., X.-Z.S., J.-J.H., X.-Q.L., C.W., X.L.).

Sources of Funding

This work was supported by grants from the National Natural Science Foundation of China (No. 81770440 to Xiang Lu, No. 81970217 and 81700331 to Wei Gao), a grant from the Natural Science Foundation of Jiangsu Province

(No. BK20171051 to Wei Gao), the Jiangsu Province Health Development Project with Science and Education (No. QNRC201685 to Wei Gao), a grant from the Six One Project of Jiangsu Province (No. LGY2018100 to Wei Gao), and a grant from the Six Talent Peaks Project of Jiangsu Province (No. WSN-175 to Wei Gao).

Disclosures

None.

Supplementary Material

Tables S1–S5

Figures S1–S2

REFERENCES

- Anderson J, Morrow D. Acute myocardial infarction. *N Engl J Med*. 2017;376:2053–2064. doi: 10.1056/NEJMra1606915
- Kolbrink B, Riebeling T, Kunzendorf U, Krautwald S. Plasma membrane pores drive inflammatory cell death. *Front Cell Dev Biol*. 2020;8:817. doi: 10.3389/fcell.2020.00817
- Xue Y, Enosi Tuipulotu D, Tan WH, Kay C, Man SM. Emerging activators and regulators of inflammasomes and pyroptosis. *Trends Immunol*. 2019;40:1035–1052. doi: 10.1016/j.it.2019.09.005
- Qi Z, Wu D, Li M, Yan Z, Yang X, Ji N, Wang Y, Zhang J. The pluripotent role of exosomes in mediating non-coding RNA in ventricular remodeling after myocardial infarction. *Life Sci*. 2020;254:117761. doi: 10.1016/j.lfs.2020.117761
- Audia JP, Yang XM, Crockett ES, Housley N, Haq EU, O'Donnell K, Cohen MV, Downey JM, Alvarez DF. Caspase-1 inhibition by VX-765 administered at reperfusion in P2Y12 receptor antagonist-treated rats provides long-term reduction in myocardial infarct size and preservation of ventricular function. *Basic Res Cardiol*. 2018;113:32. doi: 10.1007/s00395-018-0692-z
- Pang H, Wang N, Chai J, Wang X, Zhang Y, Bi Z, Wu W, He G. Discovery of novel TNN13K inhibitor suppresses pyroptosis and apoptosis in murine myocardial infarction injury. *Eur J Med Chem*. 2020;197:112314. doi: 10.1016/j.ejmech.2020.112314
- Guo M, Yan R, Yao H, Duan L, Sun M, Xue Z, Jia Y. IFN regulatory factor 1 mediates macrophage pyroptosis induced by oxidized low-density lipoprotein in patients with acute coronary syndrome. *Mediators Inflamm*. 2019;2019:2917128. doi: 10.1155/2019/2917128
- Li A, Yu Y, Ding X, Qin Y, Jiang Y, Wang X, Liu G, Chen XI, Yue ER, Sun XI, et al. MiR-135b protects cardiomyocytes from infarction through restraining the NLRP3/caspase-1/IL-1 β pathway. *Int J Cardiol*. 2020;307:137–145. doi: 10.1016/j.ijcard.2019.09.055
- Blaner WS. Retinol-binding protein: the serum transport protein for vitamin A. *Endocr Rev*. 1989;10:308–316. doi: 10.1210/edrv-10-3-308
- Yang Q, Graham TE, Mody N, Preitner F, Peroni OD, Zabolotny JM, Kotani K, Quadro L, Kahn BB. Serum retinol binding protein 4 contributes to insulin resistance in obesity and type 2 diabetes. *Nature*. 2005;436:356–362. doi: 10.1038/nature03711
- Graham TE, Yang Q, Blüher M, Hammarstedt A, Ciaraldi TP, Henry RR, Wason CJ, Oberbach A, Jansson P-A, Smith U, et al. Retinol-binding protein 4 and insulin resistance in lean, obese, and diabetic subjects. *N Engl J Med*. 2006;354:2552–2563. doi: 10.1056/NEJMoa054862
- Rychter AM, Skrzypczak-Zielinska M, Zielinska A, Eder P, Souto EB, Zawada A, Ratajczak AE, Dobrowolska A, Krela-Kazmierczak I. Is the retinol-binding protein 4 a possible risk factor for cardiovascular diseases in obesity? *Int J Mol Sci*. 2020;21:5229. doi: 10.3390/ijms21155229
- Sun HX, Ji HH, Chen XL, Wang L, Wang Y, Shen XY, Lu X, Gao W, Wang LS. Serum retinol-binding protein 4 is associated with the presence and severity of coronary artery disease in patients with subclinical hypothyroidism. *Aging*. 2019;11:4510–4520. doi: 10.18632/aging.102065
- Bobbert P, Weithäuser A, Andres J, Bobbert T, Kühl U, Schultheiss HP, Rauch U, Skurk C. Increased plasma retinol binding protein 4 levels in patients with inflammatory cardiomyopathy. *Eur J Heart Fail*. 2009;11:1163–1168. doi: 10.1093/eurjhf/hfp153
- Gao W, Wang H, Zhang L, Cao Y, Bao J-Z, Liu Z-X, Wang L-S, Yang Q, Lu X. Retinol-binding protein 4 induces cardiomyocyte hypertrophy by activating TLR4/MyD88 pathway. *Endocrinology*. 2016;157:2282–2293. doi: 10.1210/en.2015-2022

16. Elmadhun NY, Lassaletta AD, Chu LM, Sellke FW. Metformin alters the insulin signaling pathway in ischemic cardiac tissue in a swine model of metabolic syndrome. *J Thorac Cardiovasc Surg.* 2013;145:258–265; discussion 265–256. doi: 10.1016/j.jtcvs.2012.09.028
17. Gao E, Lei YH, Shang X, Huang ZM, Zuo L, Boucher M, Fan Q, Chuprun JK, Ma XL, Koch WJ. A novel and efficient model of coronary artery ligation and myocardial infarction in the mouse. *Circ Res.* 2010;107:1445–1453. doi: 10.1161/CIRCRESAHA.110.223925
18. Thirunavukkarasu M, Selvaraju V, Joshi M, Coca-Soliz V, Tapias L, Saad I, Fournier C, Husain A, Campbell J, Yee SP, et al. Disruption of VEGF mediated Flk-1 signaling leads to a gradual loss of vessel health and cardiac function during myocardial infarction: potential therapy with pellino-1. *J Am Heart Assoc.* 2018;7:e007601. doi: 10.1161/JAHA.117.007601
19. Bilbija D, Haugen F, Sagave J, Baysa A, Bastani N, Levy FO, Sirsjo A, Blomhoff R, Valen G. Retinoic acid signalling is activated in the postischemic heart and may influence remodelling. *PLoS One.* 2012;7:e44740. doi: 10.1371/journal.pone.0044740
20. Zabetian-Targhi F, Mahmoudi MJ, Rezaei N, Mahmoudi M. Retinol binding protein 4 in relation to diet, inflammation, immunity, and cardiovascular diseases. *Adv Nutr.* 2015;6:748–762. doi: 10.3945/an.115.008292
21. Abbate A, Toldo S, Marchetti C, Kron J, Van Tassel BW, Dinarello CA. Interleukin-1 and the inflammasome as therapeutic targets in cardiovascular disease. *Circ Res.* 2020;126:1260–1280. doi: 10.1161/CIRCRESAHA.120.315937
22. Pan Y, Wang L, Xie Y, Tan Y, Chang C, Qiu X, Li X. Characterization of differentially expressed plasma proteins in patients with acute myocardial infarction. *J Proteomics.* 2020;227:103923. doi: 10.1016/j.jpro.2020.103923
23. Cubedo J, Padro T, Cinca J, Mata P, Alonso R, Badimon L. Retinol-binding protein 4 levels and susceptibility to ischaemic events in men. *Eur J Clin Invest.* 2014;44:266–275. doi: 10.1111/eci.12229
24. Wang H, Zhou P, Zou D, Liu Y, Lu X, Liu Z. The role of retinol-binding protein 4 and its relationship with sex hormones in coronary artery disease. *Biochem Biophys Res Commun.* 2018;506:204–210. doi: 10.1016/j.bbrc.2018.09.159
25. Lambadiari V, Kadoglou NP, Stasinou V, Maratou E, Antoniadis A, Kolokathis F, Parissis J, Hatzigelaki E, Iliodromitis EK, Dimitriadis G. Serum levels of retinol-binding protein-4 are associated with the presence and severity of coronary artery disease. *Cardiovasc Diabetol.* 2014;13:121. doi: 10.1186/s12933-014-0121-z
26. Yang Q, Eskurza I, Kiernan UA, Phillips DA, Blucher M, Graham TE, Kahn BB. Quantitative measurement of full-length and C-terminal proteolyzed RBP4 in serum of normal and insulin-resistant humans using a novel mass spectrometry immunoassay. *Endocrinology.* 2012;153:1519–1527. doi: 10.1210/en.2011-1750
27. Thompson SJ, Sargsyan A, Lee SA, Yuen JJ, Cai J, Smalling R, Ghyselinck N, Mark M, Blaner WS, Graham TE. Hepatocytes are the principal source of circulating RBP4 in mice. *Diabetes.* 2017;66:58–63. doi: 10.2337/db16-0286
28. Welles JE, Toro AL, Sunilkumar S, Stevens SA, Purnell CJ, Kimball SR, Dennis MD. Retinol-binding protein 4 mRNA translation in hepatocytes is enhanced by activation of mTORC1. *Am J Physiol Endocrinol Metab.* 2021;320:E306–E315. doi: 10.1152/ajpendo.00494.2020
29. Sciarretta S, Forte M, Frati G, Sadoshima J. New insights into the role of mTOR signaling in the cardiovascular system. *Circ Res.* 2018;122:489–505. doi: 10.1161/CIRCRESAHA.117.311147
30. Deng Z-B, Poliakov A, Hardy RW, Clements R, Liu C, Liu Y, Wang J, Xiang X, Zhang S, Zhuang X, et al. Adipose tissue exosome-like vesicles mediate activation of macrophage-induced insulin resistance. *Diabetes.* 2009;58:2498–2505. doi: 10.2337/db09-0216
31. Mauro AG, Bonaventura A, Mezzaroma E, Quader M, Toldo S. NLRP3 inflammasome in acute myocardial infarction. *J Cardiovasc Pharmacol.* 2019;74:175–187. doi: 10.1097/FJC.0000000000000717
32. Frangiannakis NG. Pathophysiology of myocardial infarction. *Compr Physiol.* 2015;5:1841–1875. doi: 10.1002/cphy.c150006
33. Norseen J, Hosooka T, Hammarstedt A, Yore MM, Kant S, Aryal P, Kiernan UA, Phillips DA, Maruyama H, Kraus BJ, et al. Retinol-binding protein 4 inhibits insulin signaling in adipocytes by inducing proinflammatory cytokines in macrophages through a c-Jun N-terminal kinase and Toll-like receptor 4-dependent and retinol-independent mechanism. *Mol Cell Biol.* 2012;32:2010–2019. doi: 10.1128/MCB.06193-11
34. Moraes-Vieira PM, Yore MM, Sontheimer-Phelps A, Castoldi A, Norseen J, Aryal P, Simonyte Sjodin K, Kahn BB. Retinol binding protein 4 primes the NLRP3 inflammasome by signaling through Toll-like receptors 2 and 4. *Proc Natl Acad Sci USA.* 2020;117:31309–31318. doi: 10.1073/pnas.2013877117
35. Moraes-Vieira PM, Yore MM, Dwyer PM, Syed I, Aryal P, Kahn BB. RBP4 activates antigen-presenting cells, leading to adipose tissue inflammation and systemic insulin resistance. *Cell Metab.* 2014;19:512–526. doi: 10.1016/j.cmet.2014.01.018
36. Moraes-Vieira PM, Castoldi A, Aryal P, Wellenstein K, Peroni OD, Kahn BB. Antigen presentation and T-cell activation are critical for RBP4-induced insulin resistance. *Diabetes.* 2016;65:1317–1327. doi: 10.2337/db15-1696
37. Farjo KM, Farjo RA, Halsey S, Moiseyev G, Ma JX. Retinol-binding protein 4 induces inflammation in human endothelial cells by an NADPH oxidase- and nuclear factor kappa B-dependent and retinol-independent mechanism. *Mol Cell Biol.* 2012;32:5103–5115. doi: 10.1128/MCB.00820-12
38. Blaner WS. Vitamin A signaling and homeostasis in obesity, diabetes, and metabolic disorders. *Pharmacol Ther.* 2019;197:153–178. doi: 10.1016/j.pharmthera.2019.01.006
39. Kraus BJ, Sartoretto JL, Polak P, Hosooka T, Shiroto T, Eskurza I, Lee SA, Jiang H, Michel L, Kahn BB. Novel role for retinol-binding protein 4 in the regulation of blood pressure. *FASEB J.* 2015;29:3133–3140. doi: 10.1096/fj.14-266064
40. Meyers AK, Zhu X. The NLRP3 inflammasome: metabolic regulation and contribution to inflammaging. *Cells.* 2020;9:1808. doi: 10.3390/cells9081808
41. Mezzaroma E, Toldo S, Farkas D, Seropian IM, Van Tassel BW, Salloum FN, Kannan HR, Menna AC, Voelkel NF, Abbate A. The inflammasome promotes adverse cardiac remodeling following acute myocardial infarction in the mouse. *Proc Natl Acad Sci USA.* 2011;108:19725–19730. doi: 10.1073/pnas.1108586108
42. Marchetti C, Chojnacki J, Toldo S, Mezzaroma E, Tranchida N, Rose SW, Federici M, Van Tassel BW, Zhang S, Abbate A. A novel pharmacologic inhibitor of the NLRP3 inflammasome limits myocardial injury after ischemia-reperfusion in the mouse. *J Cardiovasc Pharmacol.* 2014;63:316–322. doi: 10.1097/FJC.0000000000000053
43. Marchetti C, Toldo S, Chojnacki J, Mezzaroma E, Liu K, Salloum FN, Nordio A, Carbone S, Mauro AG, Das A, et al. Pharmacologic inhibition of the NLRP3 inflammasome preserves cardiac function after ischemic and nonischemic injury in the mouse. *J Cardiovasc Pharmacol.* 2015;66:1–8. doi: 10.1097/FJC.0000000000000247
44. van Hout GP, Bosch L, Ellenbroek GH, de Haan JJ, van Solinge WW, Cooper MA, Arslan F, de Jager SC, Robertson AA, Pasterkamp G, et al. The selective NLRP3-inflammasome inhibitor MCC950 reduces infarct size and preserves cardiac function in a pig model of myocardial infarction. *Eur Heart J.* 2017;38:828–836. doi: 10.1093/eurheartj/ehw247
45. Meng Z, Song MY, Li CF, Zhao JQ. shRNA interference of NLRP3 inflammasome alleviate ischemia reperfusion-induced myocardial damage through autophagy activation. *Biochem Biophys Res Commun.* 2017;494:728–735. doi: 10.1016/j.bbrc.2017.10.111
46. Takahashi M. Cell-specific roles of NLRP3 inflammasome in myocardial infarction. *J Cardiovasc Pharmacol.* 2019;74:188–193. doi: 10.1097/FJC.0000000000000709
47. Kawaguchi M, Takahashi M, Hata T, Kashima Y, Usui F, Morimoto H, Izawa A, Takahashi Y, Masumoto J, Koyama J, et al. Inflammasome activation of cardiac fibroblasts is essential for myocardial ischemia/reperfusion injury. *Circulation.* 2011;123:594–604. doi: 10.1161/CIRCULATIONAHA.110.982777
48. Sandanger Ø, Ranheim T, Vinge LE, Bliksoen M, Afsnes K, Finsen AV, Dahl CP, Askevold ET, Florholmen G, Christensen G, et al. The NLRP3 inflammasome is up-regulated in cardiac fibroblasts and mediates myocardial ischemia-reperfusion injury. *Cardiovasc Res.* 2013;99:164–174. doi: 10.1093/cvr/cvt091
49. Liu YI, Lian K, Zhang L, Wang R, Yi FU, Gao C, Xin C, Zhu DI, Li Y, Yan W, et al. TXNIP mediates NLRP3 inflammasome activation in cardiac microvascular endothelial cells as a novel mechanism in myocardial ischemia/reperfusion injury. *Basic Res Cardiol.* 2014;109:415. doi: 10.1007/s00395-014-0415-z
50. Henderson J, Bhattacharyya S, Varga J, O'Reilly S. Targeting TLRs and the inflammasome in systemic sclerosis. *Pharmacol Ther.* 2018;192:163–169. doi: 10.1016/j.pharmthera.2018.08.003

SUPPLEMENTAL MATERIAL

Table S1. Adenovirus sequence used in the experiments

| | Adenovirus-RBP4-GFP | Adenovirus-shRBP4-EGFP |
|---------------------|--|--|
| Sequence (5'-3') | ATGGATCCTCTGGGCTGGAGAGT TTGGCTCCACCGAGACCACCCTG AGCGGAGCTCGGAGCATAGGCG ACGTGGGACGGCAAGGCTGACG GAGGGGCCCCGCGTGCCTTCAG GAGGCAGACTCCGGGGTGAGAT GGAGTGGGTGTGGGCGCTCGTG CTGCTGGCGGCTCTGGGAGGCG GCAGCGCCGAGCGCGACTGCAG GGTGAGCAGCTTCCGAGTCAAG GAGAACTTCGACAAGGCTCGTTT CTCTGGGCTCTGGTATGCCATCG CCAAAAGGACCCCGAGGGTCT CTTTTTGCAAGACAACATCATCG CTGAGTTTTCTGTGGACGAGAAG GGTCATATGAGCGCCACAGCCAA GGGACGAGTCCGTCTTCTGAGC AACTGGGAAGTGTGTGAGACAT GGTGGGCACTTTCACAGACACT GAAGATCCTGCCAAGTTCAAGA GAAGTACTGGGGTGTAGCCTCCT TTCTCCAGCGAGGAAACGATGA CCACTGATCATCGACACGGACTA CGACACCTTCGCTCTGCAGTACT CCTGCCGCCTGCAGAATCTGGAT GGCACCTGTGCAGACAGCTACTC CTTTGTGTTTTCTCGTGACCCCA ATGGCCTGAGCCCAGAGACACG GAGGCTGGTGAGGCAGCGGCAG GAGGAGCTGTGCCTAGAGAGGC AGTACAGATGGATTGAACACAAT GGTTACTGTCAAAGCAGGCCCTC CAGAAACAGTTTGTAG | CCGGTGTGGACGAGAAG GGTCATATCTCGAGATAT GACCCTTCTCGTCCACAT TTTTG |

Table S2. NLRP3-siRNA sequences used in the experiments

| | Sequence (5'-3') |
|-----------|---------------------|
| Nlrp3_001 | GTACTTAAATCGTGAAACA |
| Nlrp3_002 | CAGCCAGAGTGGAATGACA |
| Nlrp3_003 | GGATGGCTTTGATGAGCTA |

Table S3. Primers used in the experiments

| Gene | Forward primer (5' to 3') | Reverse Primer (5' to 3') |
|--------------|----------------------------------|----------------------------------|
| TBP | CCCTATCACTCCTGCCACAC | ACGAAGTGCAATGGTCTTTA GG |
| NLRP3 | TGTGAGAAGCAGGTTCTACT CT | GACTGTTGAGGTCCACACTC T |
| GSDMD | CCATCGGCCTTTGAGAAAGT G | ACACATGAATAACGGGGTTT CC |
| ASC | CTTGTCAGGGGATGAACTCA AAA | GCCATACGACTCCAGATAGT AGC |
| Caspase-1 | AGGCATGCCGTGGAGAGAAA CAA | AGCCCCTGACAGGATGTCTC CA |
| IL-1 β | GCAACTGTTCTGAACTCAA CT | ATCTTTTGGGGTCCGTCAAC T |
| IL-18 | GACTCTTGCGTCAACTTCAA GG | CAGGCTGTCTTTTGTCAACG A |
| RBP4 | AGTCAAGGAGAACTTCGACA AGG | CAGAAAACCTCAGCGATGAT GTTG |
| ANP | CCTGGAGGAGAAGATGCCGG TAGAA | CCCCAGTCCAGGGAGGCAC CTCGG |
| BNP | GAGGTCACTCCTATCCTCTGG | GCCATTTCTCCGACTTTTCT C |
| MYH7 | GAGCAAGGCCGAGGAGACG CAGCGT | GAGCCTTCTCGTCCAGCTGC CGG |

Table S4. Echocardiography indexes in mice

| Parameter | Sham(n=6) | AMI(n=6) | P value |
|---------------------------|------------------|-----------------|----------------|
| Heart Rate (BPM) | 408.77±25.98 | 427.29±29.12 | 0.648 |
| LVID;d (mm) | 3.44±0.10 | 4.34±0.16 | < 0.05 |
| LVID;s (mm) | 2.01±0.05 | 3.38±0.14 | < 0.01 |
| LV Vol;s (ul) | 13.02±0.85 | 47.65±4.84 | < 0.01 |
| LV Vol;d (ul) | 49.22±3.23 | 85.90±7.20 | < 0.01 |
| Stoke Volume (ul) | 36.20±2.67 | 38.24±4.86 | 0.716 |
| Ejection Fraction (%) | 73.39±1.36 | 44.42±3.50 | < 0.01 |
| Fractional Shortening (%) | 41.50±1.21 | 21.95±2.01 | < 0.01 |
| Cardiac Output (ml/min) | 14.73±1.32 | 16.70±2.87 | 0.551 |
| LV Mass (mg) | 104.41±8.16 | 172.73±27.40 | < 0.05 |
| LV Mass Cor (mg) | 83.53±6.53 | 138.18±21.92 | < 0.05 |
| LVPW;s (mm) | 1.33±0.04 | 1.03±0.06 | < 0.06 |
| LVPW;d (mm) | 0.87±0.04 | 0.84±0.09 | 0.788 |

Table S5. Echocardiography indexes in AMI mice injected with adenovirus

| Parameter | AMI+Ad scramble (n=7) | AMI+Ad shRBP4 (n=7) | P value |
|---------------------------|----------------------------------|--------------------------------|----------------|
| Heart Rate (BPM) | 440.29±48.58 | 463.43±27.21 | 0.29 |
| LVID;d (mm) | 4.68±0.32 | 4.33±0.23 | 0.04 |
| LVID;s (mm) | 3.81±0.30 | 3.27±0.21 | <0.01 |
| LV Vol;d (ul) | 101.82±16.12 | 84.81±10.89 | 0.04 |
| LV Vol;s (ul) | 62.76±12.05 | 43.28±6.81 | <0.01 |
| IVS;d(mm) | 0.70±0.06 | 0.72±0.14 | 0.69 |
| IVS;s(mm) | 0.9±0.11 | 0.98±0.21 | 0.59 |
| Ejection Fraction (%) | 38.53±3.32 | 49.03±2.99 | <0.01 |
| Fractional Shortening (%) | 18.63±1.81 | 24.6±1.81 | <0.01 |
| LV Mass (mg) | 132.44±23.89 | 116.83±19.63 | 0.21 |
| LV Mass Cor (mg) | 105.96±19.11 | 93.47±15.70 | 0.21 |
| LVPW;d (mm) | 0.73±0.13 | 0.71±0.05 | 0.81 |
| LVPW;s (mm) | 0.96±0.14 | 1.02±0.08 | 0.34 |

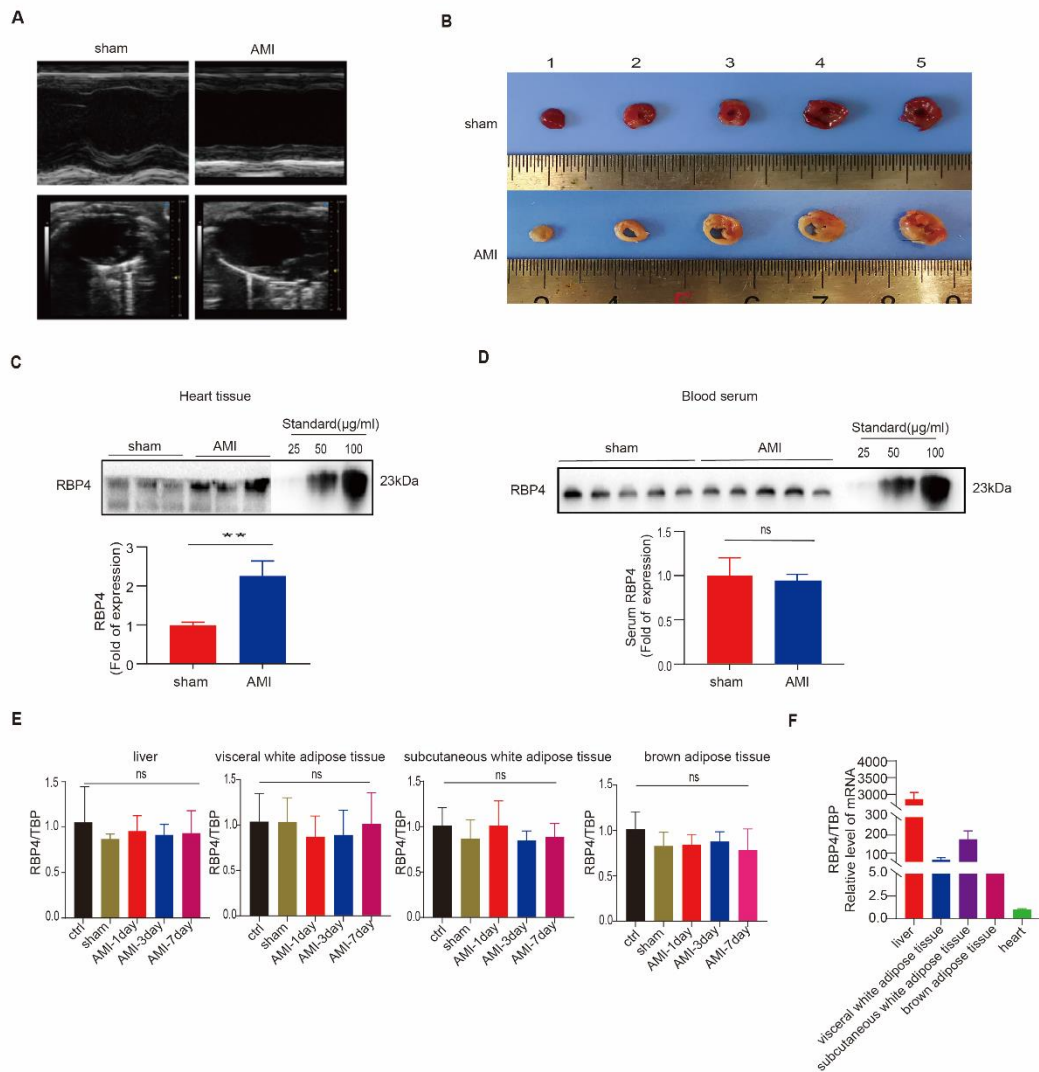


Figure S1. Mice model of AMI. (A) Echocardiography showing that the left ventricular end-diastolic diameter and left ventricular end-systolic diameter were increased in mice with AMI compared to sham controls. (B) TTC staining of myocardium in AMI mice and sham controls. (C) Quantitative western blot determination of the relative content of RBP4 protein in heart tissue using purified mouse RBP4 for generating the standard curves. (D) Quantitative western blot determination of the relative content of RBP4 protein in serum using purified mouse RBP4 for generating the standard curves. (E) mRNA levels of RBP4 in liver, visceral white adipose tissue, subcutaneous white adipose tissue, and brown adipose tissue. ns, no significance. (F) Comparison of RBP4

mRNA levels in different tissues under normal condition. n = 6 per group; **, $P < 0.05$

vs. sham; ns, no significance.

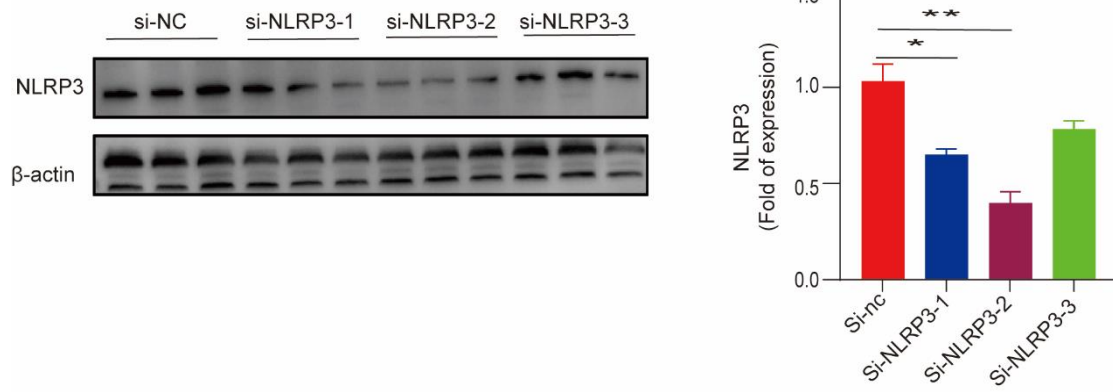


Figure S2. Verify the efficiency of NLRP3 small interference RNAs by western blot.

n = 3; * $P < 0.05$ vs. NC, ** $P < 0.01$ vs. NC.